Timing of Tissue-specific Cell Division Requires a Differential Onset of Zygotic Transcription during Metazoan Embryogenesis

Wong, Ming-Kin; Guan, Daogang; Ng, Kaoru Hon Chun; Ho, Vincy Wing Sze; An, Xiaomeng; Li, Runsheng; Ren, Xiaoliang; Zhao, Zhongying

Published in:
Journal of Biological Chemistry

Published: 10/06/2016

Document Version:
Final Published version, also known as Publisher's PDF, Publisher's Final version or Version of Record

Published version (DOI):
10.1074/jbc.M115.705426

Publication details:
Wong, M.-K., Guan, D., Ng, K. H. C., Ho, V. W. S., An, X., Li, R., Ren, X., & Zhao, Z. (2016). Timing of Tissue-specific Cell Division Requires a Differential Onset of Zygotic Transcription during Metazoan Embryogenesis. *Journal of Biological Chemistry*, *291*(24), 12501-12513. https://doi.org/10.1074/jbc.M115.705426

THE JOURNAL OF BIOLOGICAL CHEMISTRY VOL. 291, NO. 24, pp. 12501–12513, June 10, 2016

Timing of Tissue-specific Cell Division Requires a Differential Onset of Zygotic Transcription during Metazoan Embryogenesis*[S]

Received for publication, November 19, 2015, and in revised form, March 28, 2016 Published, JBC Papers in Press, April 7, 2016, DOI 10.1074/jbc.M115.705426

Ming-Kin Wong[‡], Daogang Guan[‡], Kaoru Hon Chun Ng[‡], Vincy Wing Sze Ho[‡], Xiaomeng An[‡], Runsheng Li[‡], Xiaoliang Ren[‡], and Zhongying Zhao[‡§1]

From the [‡]Department of Biology, Hong Kong Baptist University and the [§]State Key Laboratory of Environmental and Biological Analysis, Hong Kong Baptist University, Hong Kong, China

Metazoan development demands not only precise cell fate differentiation but also accurate timing of cell division to ensure proper development. How cell divisions are temporally coordinated during development is poorly understood. *Caenorhabditis elegans* embryogenesis provides an excellent opportunity to study this coordination due to its invariant development and widespread division asynchronies. One of the most pronounced asynchronies is a significant delay of cell division in two endoderm progenitor cells, Ea and Ep, hereafter referred to as E2, relative to its cousins that mainly develop into mesoderm organs and tissues. To unravel the genetic control over the endoderm-specific E2 division timing, a total of 822 essential and conserved genes were knocked down using RNAi followed by quantification of cell cycle lengths using *in toto* imaging of *C. elegans* embryogenesis and automated lineage. Intriguingly, knockdown of numerous genes encoding the components of general transcription pathway or its regulatory factors leads to a significant reduction in the E2 cell cycle length but an increase in cell cycle length of the remaining cells, indicating a differential requirement of transcription for division timing between the two. Analysis of lineage-specific RNA-seq data demonstrates an earlier onset of transcription in endoderm than in other germ layers, the timing of which coincides with the birth of E2, supporting the notion that the endoderm-specific delay in E2 division timing demands robust zygotic transcription. The reduction in E2 cell cycle length is frequently associated with cell migration defect and gastrulation failure. The results suggest that a tissue-specific transcriptional activation is required to coordinate fate differentiation, division timing, and cell migration to ensure proper development.

Proper development of metazoans depends not only on precise differentiation of cell fate but also on tight control over division timing or division pace between cells, which we refer to as temporal coordination. A normal fate specification without correct division timing may lead to catastrophes, for example, cancerous development (1). Therefore, metazoan development demonstrates stereotyped division timing (2, 3). Despite intensive studies on the regulation of cell fate differentiation, genetic control over temporal coordination of cell division during metazoan development is poorly understood. Timing of cell division is particularly critical during early developmental stages such as embryogenesis when cells undergo rapid division and migration, which is concomitant with cell fate differentiation.

Because of technical challenges in quantifying cell division timing especially when an embryo undergoes rapid cell division, most of the studies on cell division timing focus on the earliest stage of development (4). For example, the first embryonic division in *Caenorhabditis elegans* produces two daughters, namely AB and P1, with differential developmental potential. The two cells also divide asynchronously with the former dividing approximately 2 min earlier than the latter (2). Maternally provided PAR proteins were found to regulate the asynchrony by controlling the timing of mitotic entry and the rate of DNA replication (5, 6). Recent developments in live cell imaging and automated cell tracking have greatly facilitated systematic and accurate measurement of cell division timing during entire or partial embryogenesis (7–9), which allows for identification of genes that control temporal coordination of cell division during metazoan embryogenesis. We have recently performed a reverse genetic screening using the highly conserved and essential genes and looked for those whose perturbation produces a significant reduction in division asynchrony between sibling cells developing into the same or distinct cell types (10). The results demonstrate that both fate asymmetry and asynchrony are controlled by a similar genetic scheme, raising the possibility that division timing could be an integral part of cell fate differentiation. However, in addition to the asynchrony between sibling cells, cell division timing also demonstrates a lineal or tissue-specific dependence. How cell divisions are timed in a lineal or tissue-specific fashion remains poorly understood.

C. elegans embryogenesis provides an excellent opportunity for illustrating the genetic control over the lineal or tissue-specific division timing because of its invariant development. Unlike embryogenesis of vertebrate and *Drosophila* species where the initial rounds of cell division are synchronized (11),

* This work was supported by Collaborative Research Fund HKBU5/CRF/11G and Early Career Scheme Fund HKBU263512 from Hong Kong Research Grant Council (to Z. Z.). The authors declare that they have no conflicts of interest with the contents of this article. The content is solely the responsibility of the authors and does not necessarily represent the official views of the National Institutes of Health.

[S] This article contains supplemental Figs. S1–S3, Movies S1 and S2, and Table S1 and S2.

[1] To whom correspondence should be addressed: Dept. of Biology, Hong Kong Baptist University, Hong Kong, China. Tel.: 852-3411-7058; E-mail: zyzhao@hkbu.edu.hk.

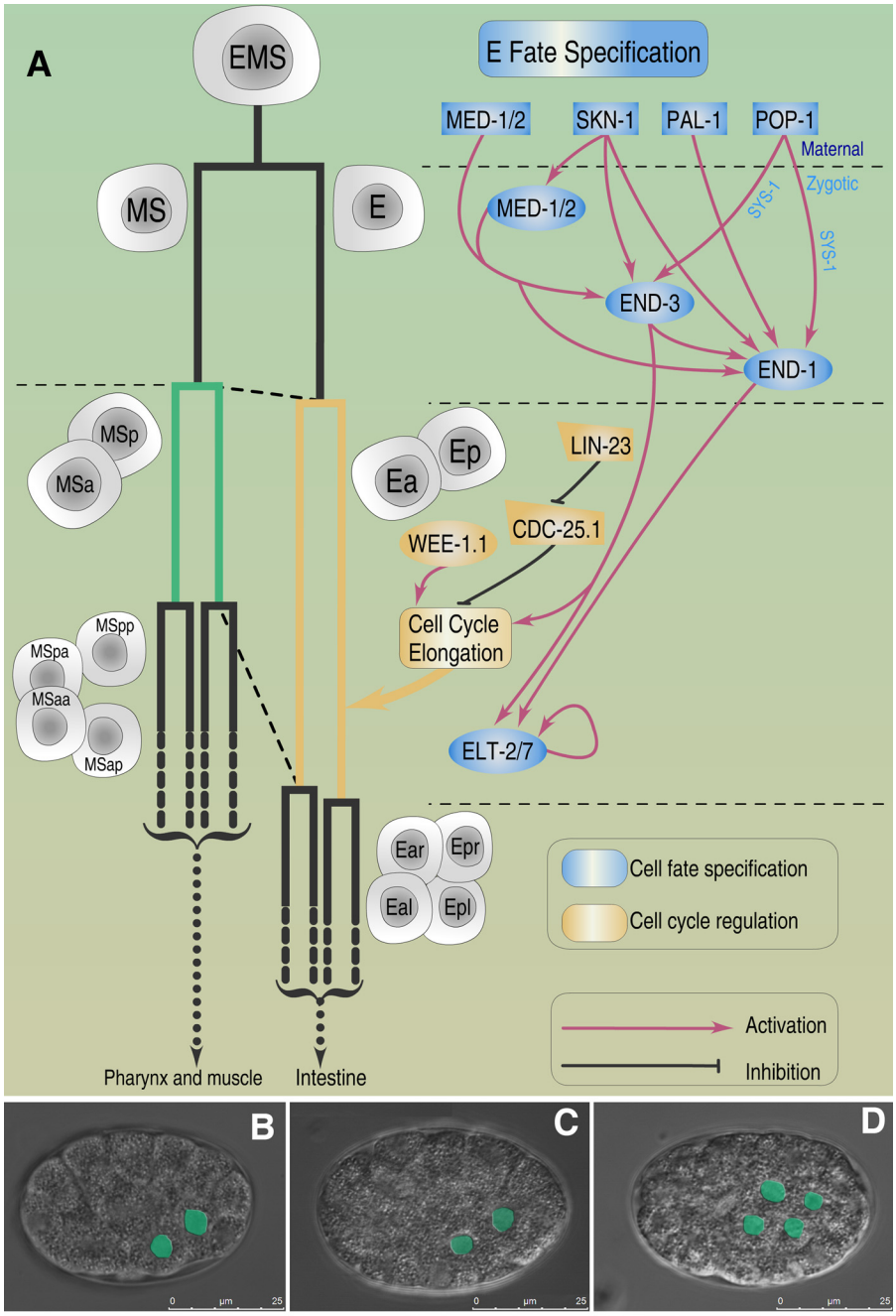

FIGURE 1. **Genetic pathways controlling endoderm specification and cell cycle control.** *A,* summary of current understanding of genetic pathways controlling fate specification (*blue*) and cell cycle length (*brown*) of E lineage. E fate specification is under combinatorial control by maternal factors and Wnt signaling pathway as denoted by POP-1, which drives the expression of two redundant E fate specifiers, END-1 and END-3. The two factors in turn up-regulate intestine-specific transcription factors, ELT-2 and ELT-7. Cell cycle lengths are highlighted in *brown* and *green* for E2 and MS2, respectively. *B–D,* differential interference contrast micrographs of a developing embryo before (*B*) or after gastrulation (*C* and *D*). Progeny of E are *highlighted*.

C. elegans embryogenesis demonstrates widespread asymmetries in cell division throughout embryogenesis (2, 10). One of the most prominent asynchronies is a significant delay in division of intestine progenitors, E2 (Ea and Ep cells), relative to their cousins from other lineal origins during *C. elegans* embryogenesis (Fig. 1). At this stage, cell division is believed mainly controlled by maternal factors (12, 13) except for E (14). E is the only lineage that gives rise to endoderm, and the development is clonal, *i.e.* no other tissue types are derived from the E lineage (2). Average cell cycle length of E2 is ~40 min, while that for their cousins of MS lineage (MSa and MSp) is roughly 20 min at 20 °C (Figs. 1 and 2*A*) (10). Previous studies on gastrulation demonstrated that an inhibition of RNA polymerase II activity by its antisense RNA (13) or temperature-sensitive mutation in an uncharacterized protein, GAD-1, resulted in gastrulation failure and precocious division of E2 (15). E fate specification also plays an important role in regulating the cell cycle length. Perturbation of E specification is frequently associated with extra rounds of cell divisions, which is due to an accelerated division pace and fate transformation from E to

MS- or C-like fates (16–19). Single molecular RNA imaging combined with automated lineage study suggested that expression of fate markers in endoderm is independent of its division timing (20). However, a systematic analysis of how the division of E2 cells is specifically delayed compared with those of the remaining cells is still lacking. To this end, we took advantage of a large collection of data on cell cycle length that we generated upon perturbation of 822 essential and conserved genes using automated lineage (10). We found that in contrast to the cell cycle of the other lineages, an E2-specific increase in cell cycle length requires a robust activation of zygotic transcription, which may also be important for proper cell migrations.

Materials and Methods

Worm Strains and Maintenance—The following strains were used: N2, RW10226 (*unc-119*(*ed3*)) III; *stIs10226*[*his-72* promoter::HIS-24::mCherry::let-858 3′ UTR + *unc-119*(+)]; *itIs37* [*pie-1* promoter::mCherry::H2B::*pie-1* 3′UTR + *unc-119*(+)], RW10425 (*stIs10226* [*his-72* promoter::HIS-24::mCherry::*let-858* 3′ UTR + *unc-119*(+))]; *itIs37* [*pie-1* promoter::*mCherry*::H2B::*pie-1 3′UTR* + *unc-119*(+)]; *stIs10389* [PHA-4::TGF(3E3)::GFP::TY1::3×FLAG]; RW10348 (*stIs10226* [*his-72* promoter::HIS-24::mCherry::*let-858* 3′ UTR + *unc-119*(+)); *itIs37* [*pie-1* promoter::mCherry::H2B::*pie-1 3′UTR* + *unc-119*(+)]; *stIs10318* [NHR-25::TGF(3H4)::GFP::TY1::3×FLAG]; RW10234 (*zuIs178* [*his-72* promoter::HIS-72::GFP::*his-72* 3′ UTR + *unc-119*(+)], *stIs*10024 [*pie-1* promoter::H2B::GFP::*pie-1* 3′ UTR + *unc-119*(+)]; stIs10220 [*end-1* promoter::H1-mCherry + *unc-119*(+)]) and RW10481 (*stIs10226* [*his-72* promoter::HIS-24::mCherry::let-858 3′ UTR + *unc-119*(+)]; *itIs37* [*pie-1* promoter::mCherry::H2B::*pie-1 3′UTR* + *unc-119*(+)]; *stIs10436* [*hlh-1* promoter::TGF(6.2B4)::GFP::TY1::3×FLAG]) as described previously (10). *wee-1.1* deletion strain RB669 was used for determining the genetic interaction between *wee-1.1* and other genes as stated below. All the animals were maintained on NGM plate seeded with *Escherichia coli* OP50 at room temperature (25 °C).

RNA Interference—Gene prioritization was described previously (10). Briefly, only genes that have a clear human ortholog and produce lethal phenotypes upon perturbation were screened for defects in division timing. Genes whose perturbation produced early embryonic arrest were excluded from further analysis. Gene-specific primers were picked, and RNAi was performed through microinjection as described (21). All the primer sequences were deposited in Phenics database.

Imaging, Automated Lineaging, and Gene Expression Profiling—In toto imaging was performed with an inverted Leica SP5 confocal microscope equipped with two hybrid detectors at a constant ambient temperature of 20 °C. Images were consecutively collected for both GFP and mCherry channels every 90 s from 41 focal planes for a total of 6 h. For each gene perturbation, images were collected for at least three replicate embryos. Automated lineage and gene expression profiling were performed as described (22). Wild-type embryos were curated up to ~350-cell stage for all wild-type embryos and to the equivalent stage or to the last editable stage for all the perturbed embryos by RNAi. At least two replicated embryos were curated.

Manual Measurement of Cell Cycle Length—Time-lapse differential interference contrast imaging was performed in the same way as that for fluorescence imaging. For strains carrying a temperature-sensitive allele, a young adult or L4 animal was raised at 25 °C overnight followed by embryo retrieval and imaging. The differential interference contrast images were converted into StarryNite compatible format and fed into AceTree for visualization and manual measurement of cell cycle length by manually tracing the E2 cell from its birth to division.

Statistical Analysis on Cell Cycle Length—Cell cycle lengths for all wild-type and perturbed embryos were computed with StarryNite (7) and deposited in the Phenics database. Average cell lengths for 91 wild-type embryos were previously calculated up to ~350-cell stage (10). To identify genes whose perturbation produces a significant deviation from wild-type average, D'Agostino's K^2 test was performed as described previously (10) to evaluate the distribution of individual E2 cell cycle lengths between 91 wild-type embryos. At least 75.8% of all examined lengths passed the normality test with an α value of 0.05, which allowed us to assign the probability of E2 cell cycle length of a perturbed embryo outside the 95 and 99% confidence interval of the distribution of wild-type E2 cell cycle length as the p value of $p < 0.05$ and $p < 0.01$, respectively. Significant effects are declared only upon observation of at least two statistically significant ($p < 0.05$ and $p < 0.01$) repeats from perturbation of a single gene.

Hierarchical Clustering of E2 Cell Cycle Length—Genes whose perturbation produced a significant ($p < 0.01$) increase or decrease in E2 cell cycle were pooled together to build a matrix consisting of cell cycle lengths. Only genes whose perturbation produced a significant change in at least two embryos were retained for further analysis. Specifically, cell cycle lengths of E2 as well as 12 other cells that are present at the same generation as E2 were collected, including those from MS2 (MSa and MSp), C2 (Ca and Cp), and AB8 (ABala, ABalp, ABara, ABarp, ABpla, ABplp, ABpra, and ABprp). Average fold change in cell cycle length between replicate embryos *versus* average cell cycle length of 91 wild-type embryos were computed for each gene. The resulting matrix was used as an input for clustering analysis, which was implemented in R with "heatmap.2" function in "gplots" package by using the Ward D "Minkowski" distance measure (Fig. 4*B*).

Mining and Analysis of C. elegans Blastomere-specific RNA Sequencing Data—Blastomere cell-specific RNA-seq[2] data over developmental time were downloaded from Gene Expression Omnibus (GEO) with accession number GSE50548 produced previously (23). Normalized transcript abundance (number of transcripts per million reads) of each blastomere was retrieved for all genes, which were divided into three germ layer-specific categories based on the tissue-specific SAGE data (24). RNA-seq from blastomere E, AB, and MS were used as a proxy for endoderm, ectoderm, and mesoderm, respectively. Developmental time was aligned against E, E2, E4, E8, when E and progeny are available. Alignment to P1 and EMS was used before E was born as described (23).

[2] The abbreviations used are: RNA-seq, RNA sequencing; AP, anterior-posterior; LR, left-right; DV, dorsal-ventral; N/C, nucleus and cytoplasm.

Data Analysis on Cell Migration—Statistical analysis of division angles and positions was performed as described previously (10). Division angles were computed against three reference planes defined by the following axes, *i.e.* anterior, posterior (AP)-left, right (LR), dorsal, ventral (AP-DV), and LR-DV, respectively. Normality of the division angles and cell positions in all 91 wild-type embryos were examined with D'agostino's K^2 test. For position, 72.2% of the values passed the test when an α value of 0.05 was used. For division angle, the ratios of normally distributed angles were 93.6, 84.2, and 75.1% against planes defined by AP-LR, LR-DV, and AP-DV, respectively, with a cutoff α value of 0.05. The means and standard deviations were computed for angle distribution of wild-type embryos. A significant deviation from wild-type distribution for the cell migration of a perturbed embryo was assigned a p value of 0.01 and 0.05, respectively, for the probability that falls outside the 99 and 95% confidence interval of the wild-type distribution. Visualization of three-dimensional projection of cell migration was generated as described previously (10).

Genetic Interaction between wee-1.1 and the Components of General Transcriptional Machinery—Allele *wee-1.1* (*ok418*) was crossed with N2 five times to reduce background mutations. The presence or absence of the allele was examined by genotyping using single worm PCR with primers of the following sequences: ok418_ext2-L, ACCGATCTCATGTCCGAAATT, and ok418_ext2-R, ATGGCAGCTCACAAACTTGG; ok418_int2-L, GTGTCCATATGCTTCGCGATA, and ok418_int2-R, ACATACATTCTCCGACGAAATGA. The allele was crossed into the lineage strain RW10226 (8) and rendered homozygous along with lineage markers to give rise to the strain ZZY505, which was used for measurement of cell cycle length with or without perturbation of components of general transcription machinery by automated lineage.

Results

Genes with a Significantly Shortened E2 Cell Cycle Length upon Perturbation Are Predominantly the Components of General Transcription Pathway or Its Regulators—To identify genes that regulate E2 cell cycle length, we have established a pipeline consisting of gene knockdown with RNAi through microinjection, *in toto* imaging of *C. elegans* embryogenesis, and automated lineaging (7, 10). We first measured cell cycle length for all cells up to the 350-cell stage for a total of 91 wild-type embryos. We next prioritized a total of 822 genes to be included in the pipeline based on their conservation and reported phenotypes upon perturbation. We performed RNAi by injection on all prioritized genes and screened for those whose perturbation produced a significant decrease or increase ($p < 0.01$) in E2 cell cycle length against the average cell cycle length of the 91 wild-type embryos. Only genes with at least two embryos showing a reproducible change were included for the subsequent analysis. In most cases, the strain used for RNAi is RW10425 (25), which expresses PHA-4 as a cell fate marker. Lineaging results were curated up to the 350-cell stage for the wild-type and perturbed embryos. A subset of perturbed embryos was curated to the last editable time point because the perturbed embryos arrested before developing into the 350-cell stage. Cell cycle lengths for all wild-type and perturbed embryos were deposited into the Phenics database.

We classified the significant changes in E2 cell cycle length into two categories, *i.e.* increase and decrease in cell cycle length. Intriguingly, most genes that produced a significant reduction in E2 length upon perturbation encode the components of general transcription machinery or its regulators (Fig. 2*B* and Table 1). For example, a total of 30 out of the 53 genes that show a significant reduction in E2 cell cycle length ($p < 0.01$) are those directly involved in general transcription, including two encoding subunits of RNA polymerase II, six involved in transcriptional initiation, one in transcriptional elongation, 17 in RNA splicing, three in poly(A) binding, and one in mRNA export and stability. For example, knockdown of *rbpl-1*, which encodes a protein predicted to be involved in mRNA poly(A) tailing, shortens E2 cell cycle length by 38.8% (Fig. 2*A*). Most of the remaining genes encode regulatory proteins, including five components of Wnt signaling pathway, two transcription factors, and three chromatin modifiers. Involvement of the Wnt pathway in regulation of E2 cell cycle length is not surprising because knockdown of the pathway was found to cause fate transformation from E into MS-like fate, which is coupled with shortened cell cycle lengths (26). *ada-2* and *cbp-1* are predicted to encode proteins with histone acetyltransferase activity (27), which is important for initiation of gene expression. Also expected are maternal factors known to be required for E lineage specification, including SKN-1, PAR-2, and CUL-1. Depletion of SKN-1 was known to lead to fate transformation from E to a C-like fate (16), and knockdown of the latter two results in transformation from E to a MS-like cell (28).

Cell Cycle Lengths Are Differentially Regulated between E2 and Other Cells—Given a global coupling of developmental speed and transcription timing during *C. elegans* embryogenesis (20), we wondered whether an inhibition of gene activities leading to a significant reduction in E2 cell cycle length produces a similar effect in other cells. To this end, we first pooled cell cycle lengths for all cells roughly at the same generation as E2 cells for two categories of genes, *i.e.* those whose perturbation produced a significant decrease or increase (both $p < 0.01$) in average E2 cell cycle length compared with that of wild-type average. We next performed clustering analysis for all the cell cycle lengths with fold change of the cell cycle length *versus* the average of wild type as an input. Surprisingly, nearly all of the perturbations that produced a significant decrease in E2 cell cycle length led to an increased cell cycle length in the remaining cells (Fig. 3*A*). In contrast, perturbations that produced a significant increase in E2 cell cycle length also caused an increased cell cycle length in the remaining cells. It is intriguing that most of the latter genes are not directly involved in mRNA production but are involved in energy production, protein translation or trafficking, and transcriptional regulation such as transcription factor (supplemental Table S1). The remaining ones include those involved in cell adhesion, cytoskeleton organization, and chromatin modification. However, the scale of fold change in cell cycle length is not comparable between the categories of cell cycle length increase and decrease (Table 1 and supplemental Table S1). It is not clear why interference of

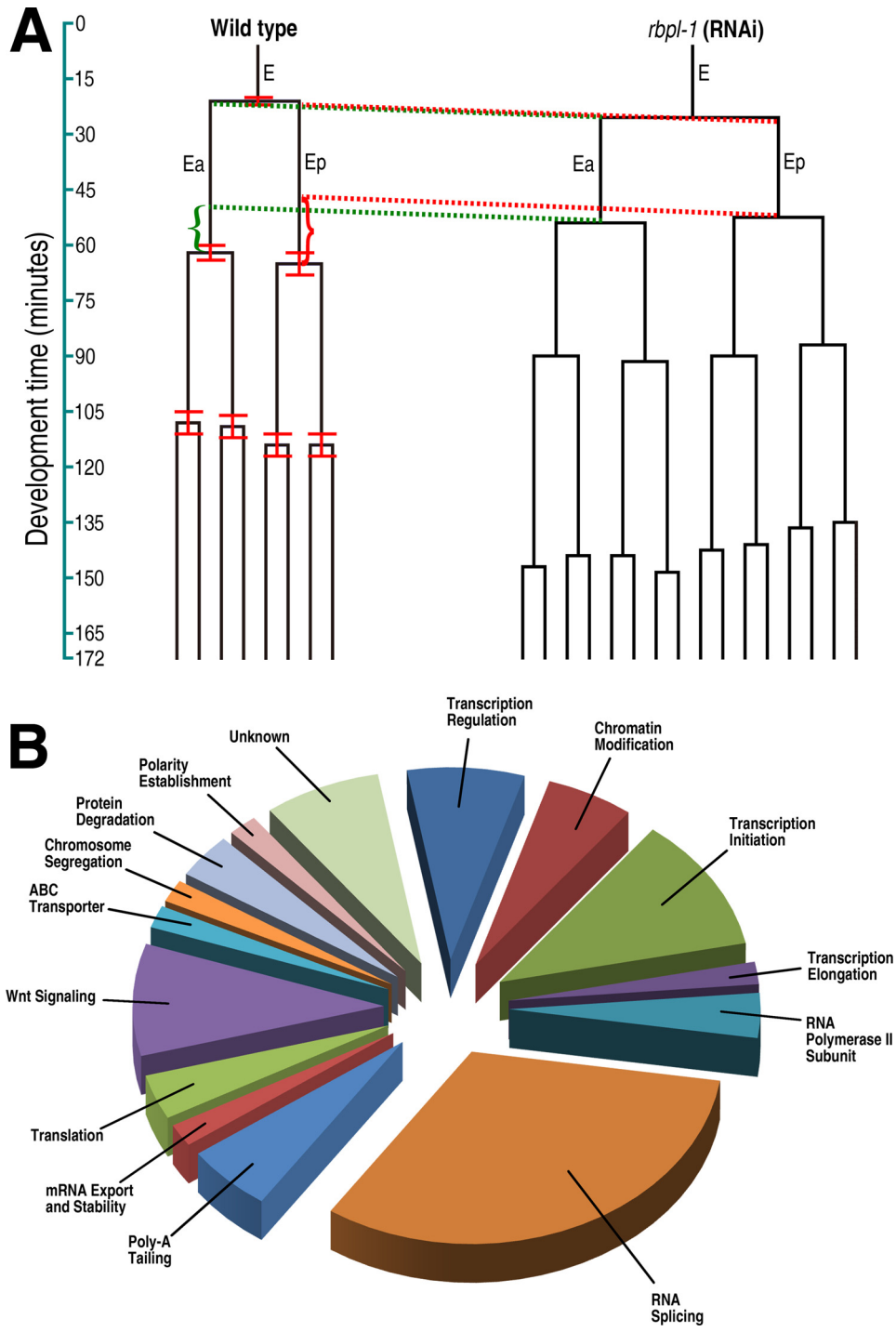

FIGURE 2. **Ontology of genes whose perturbation produces a significant reduction ($p < 0.01$) in E2 cell cycle length compared with wild type.** *A,* lineal comparison of E cell division timing between a wild-type average (*left*) and an *rbpl-1* RNAi embryo. Embryo development time starting from the last time point of "ABal" is shown on the *left*. Standard deviations of cell cycle lengths from 91 wild-type embryos are indicated in *red* for E2 and E4. Equivalent E2 cell cycle lengths are highlighted with *dashed lines* between wild-type average and the perturbed embryo. *B, pie chart* showing the ontology of all genes with a significant reduction in E2 cell cycle length ($p < 0.01$). Note nearly 60% of the genes function on the pathways of mRNA production and stability.

zygotic transcription or protein translation produces an opposite effect on E2 cell cycle length.

To illustrate E2 cell cycle control at a systems level, we contrasted cell cycle lengths for all cells in both wild-type and perturbed embryos with two genes. One is *rbpl-1* that encodes a putative mRNA poly(A)- binding protein, and the other is *wee-1.1* that encodes a homolog of cell cycle-regulating Ser/Thr kinase *Wee1* in yeast as well as *wee1/2* in humans, where it functions as an integral component of the G_2/M checkpoint by controlling the dynamics of the cell cycle oscillator (29). The latter is included because a previous study indicated its specific role in E2 cell cycle control (30) and is known to be a zygotic target of MED-1 and MED-2 in the *C. elegans* embryo (31). As stated above, knockdown of *rbpl-1* led to an opposite change in

TABLE 1

List of genes whose perturbation leads to a significant reduction in E2 cell cycle length ($p < 0.01$)

Only genes with at least two reproducible replicates were used for calculation of cell cycle length.

Gene name	Cell cycle length	Pathway	Description
	min		
Wild type	42.5	Not applicable	Not applicable
pie-1	35.7	Maternal	C-*X*8-C-*X*5-C-*X*3-H-type zinc finger protein
skn-1	32.4	Maternal	bZip transcription factor (maternal)
par-2	25.4	Maternal	Protein containing a C3HC4-type RING-finger found in E3 ubiquitin ligase subunits
cul-1	34.2	Protein degradation	Cullin, orthologous to Cdc53/Cul1 in *Saccharomyces cerevisiae* and CUL-1 in humans
skr-2	32.8	Protein degradation	A homolog of Skp1 in *S. cerevisiae*, a core component of the SCF (Skp1p, Cullin, F-box) ubiquitin-ligase complex that facilitates ubiquitin-mediated protein degradation
apr-1	33.3	Wnt signaling	Ortholog of human APC
gsk-3	27.2	Wnt signaling	Glycogen synthase kinase involved in Wnt signaling
lit-1	23.1	Wnt signaling	Serine/threonine protein kinase
mom-2	32.9	Wnt signaling	Member of the Wnt family of secreted signaling glycoproteins
wrm-1	23.1	Wnt signaling	One of three *C. elegans* β-catenin-like proteins, involved in Wnt signaling
odd-2	35.2	Transcriptional regulation	Homolog of zinc finger transcription factor
sbp-1	32.0	Transcriptional regulation	Basic helix-loop-helix (bHLH) transcription factor
ada-2	31.3	Chromatin modification	Histone acetyltransferase complex (subunit)
cbp-1	24.2	Chromatin modification	Homolog of the mammalian transcriptional cofactors CBP and p300 that have been shown to possess histone acetyltransferase activity
swsn-1	23.5	Chromatin modification	An ortholog of SWI3, a component of the SWI/SNF complex that is conserved from yeast to mammals and that is involved in chromatin remodeling
cyh-1	34.3	Transcriptional initiation	Cyclin-H associated with protein kinase Kin28p, which is the TFIIH-associated C-terminal domain (CTD) kinase in *S. cerevisiae*
taf-1	31.3	Transcriptional initiation	Ortholog of human TATA-binding protein associated factor TAF1L
taf-4	32.0	Transcriptional initiation	Isoform 1 of transcription initiation factor TFIID subunit 4B in *H. sapiens*
Y39B6A.36	34.5	Transcriptional initiation	General transcription factor IIF subunit 2 in *Homo sapiens*
Y66D12A.15	28.2	Transcriptional initiation	Component of the holoenzyme form of RNA polymerase transcription factor TFIIH in *S. cerevisiae*; TFIIH basal transcription factor complex helicase XPB subunit in *H. sapiens*
ZK1128.4	31.3	Transcriptional initiation	Subunit of TFIIH complex, involved in transcription initiation in *H. sapiens*
cdk-9	29.2	Transcriptional elongation	Ortholog of the metazoan transcription elongation factor kinase CDK-9
ama-1	29.3	RNA polymerase II subunit	Large subunit of RNA polymerase II
rpb-3	23.2	RNA polymerase II subunit	RNA polymerase II (B) subunit
cyl-1	23.2	RNA splicing	Non-coding transcript isoform; isoform 1 of cyclin-L1 in *H. sapiens*
F10B5.8	33.8	RNA splicing	Subunit of the mRNA cleavage and polyadenylation specificity complex in *S. cerevisiae*
F19F10.12	32.4	RNA splicing	Integrator complex subunit 9 in *H. sapiens*
mog-1	34.2	RNA splicing	DEAH helicase
mog-4	26.4	RNA splicing	Putative pre-mRNA-splicing factor ATP-dependent RNA helicase DHX16 in *H. sapiens*
mog-5	21.1	RNA splicing	A DEAH helicase orthologous to the *S. cerevisiae* PRP22 proteins
D1081.8	23.3	RNA splicing	Splicing factor in *S. cerevisiae*; cell division cycle 5-like protein in *H. sapiens*
F19F10.9	21.1	RNA splicing	Component of the U4/U6.U5 snRNP complex in *S. cerevisiae*
F53B7.3	21.8	RNA splicing	Isoform 2 of pre-mRNA-splicing factor ISY1 homolog in *H. sapiens*
let-858	22.2	RNA splicing	Nucampholin
M03F8.3	20.4	RNA splicing	Isoform 1 of Crooked neck-like protein 1 in *H. sapiens*
plrg-1	19.4	RNA splicing	Plrg-1 (pleiotropic regulator (vertebrate) homolog); isoform 2 of pleiotropic regulator 1 in *H. sapiens*; member of the NineTeen Complex (NTC) in *S. cerevisiae*
prp-38	33.4	RNA splicing	Isoform 1 of pre-mRNA-splicing factor 38A in *H. sapiens*; nucleolar protein in *S. cerevisiae*
prp-8	22.5	RNA splicing	Component of the U4/U6-U5 snRNP complex in *S. cerevisiae*
repo-1	32.6	RNA splicing	Subunit of the SF3a splicing factor complex in *S. cerevisiae;* SF3A2 protein in *H. sapiens*
stip-1	30.3	RNA splicing	Essential protein that forms a dimer with Ntr2p in *S. cerevisiae*
T10C6.5	27.7	RNA splicing	Spliceosome-associated protein CWC15 homolog in *Pongo abelii*
cpsf-2	32.6	Poly(A) tailing	Cleavage and polyadenylation specificity factor
pfs-2	32.7	Poly(A) tailing	Polyadenylation factor subunit homolog
rbpl-1	25.5	Poly(A) tailing	May regulate gene expression as an mRNA cleavage and polyadenylation factor
ncbp-1	35.2	mRNA export and stability	A putative nuclear cap-binding complex subunit
ddx-23	34.9	Translation	Essential ATP-dependent RNA helicase of the DEAD-box protein family, involved in nonsense-mediated mRNA decay and rRNA processing in *S. cerevisiae*
eftu-2	23.2	Translation	Elongation factor 2 (EF-2)-like protein
R08D7.1	19.7	Chromosome segregation	Subunit of the condensin complex in *S. cerevisiae*
pgp-9	34.5	ABC transporter	Member of the ATP-binding cassette (ABC) transporter superfamily
cacn-1	21.1	Unknown	An ortholog of *Drosophila* CACTIN and human C19orf29; Putative positive regulator of mannosyl-phosphate transferase (Mnn6p) in *S. cerevisiae*
cir-1	20.4	Unknown	A nuclear protein homologous to mammalian CIR
gad-1	27.5	Unknown	WD repeat-containing protein
tads-1	24.8	Unknown	Limited homolog to DNA replication termination factor

cell cycle length between E progeny (but not E itself), and those from the remaining lineages, *i.e.* a significantly faster division pace of E progeny but an apparent slowdown in the progeny of remaining lineages compared with the wild type (Fig. 3*B*), suggesting a differential requirement of gene transcription between E progeny and the remaining cells as well as E itself. Such a change is traditionally described as a fate transformation from E into MS-like mostly based on division pattern. However, this

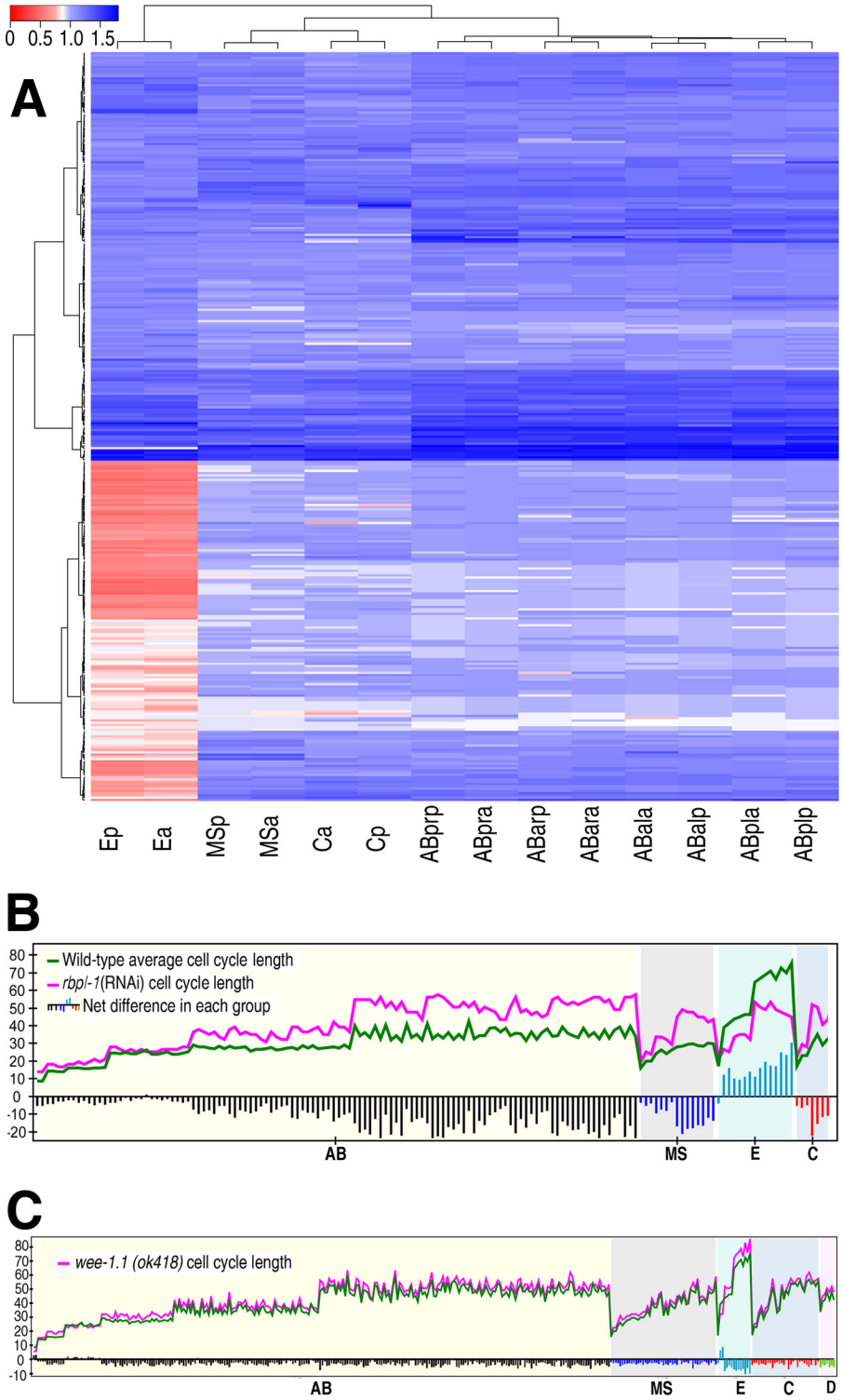

FIGURE 3. **Differential regulation of cell cycle length between E2 and the remaining cells of the similar stage.** *A,* clustering analysis of average fold changes in E2 (Ea and Ep) and other cells derived from AB, MS, and C that are approximately in the same generation. Only the RNAi experiments producing significant changes in E2 cell cycle length as opposed to wild type ($p < 0.01$) were included for clustering (see "Materials and Methods" for details). Note an opposite change pattern between E2 faster (*red*) and the remaining categories (*blue*) by perturbation of a subset of genes, *i.e.* perturbations lead to an expanded cell cycle length in most cells except E2. *B* and *C,* pairwise comparison of cell cycle length for cells between wild-type average and an *rbpl-1*(RNAi) (*B*) or a *wee-1.1*(ok418) embryo (*C*). The *x* axis denotes the origin of cells ordered alphabetically based on its name, and *y* axis denotes the net difference in cell cycle length between the mutant/RNAi and wild type in minute. Knockdown of *rbpl-1* results in a reduction of cell cycle length for E progeny except for itself. Note a greater change in E2 than in other E progeny. A loss-of-function mutation in WEE-1.1 leads to an E2-specific reduction in cell cycle length.

description is apparently not accurate in terms of cell fate (see below). Inhibition of *wee-1.1* activities resulted in an E2-specific reduction in cell cycle length (Fig. 3*C*), which is consistent with the previous results (30). A tissue-specific reduction in cell cycle length upon *wee-1.1* perturbation is surprising in that the protein is not only expressed in E at the 12–16-cell stage, but

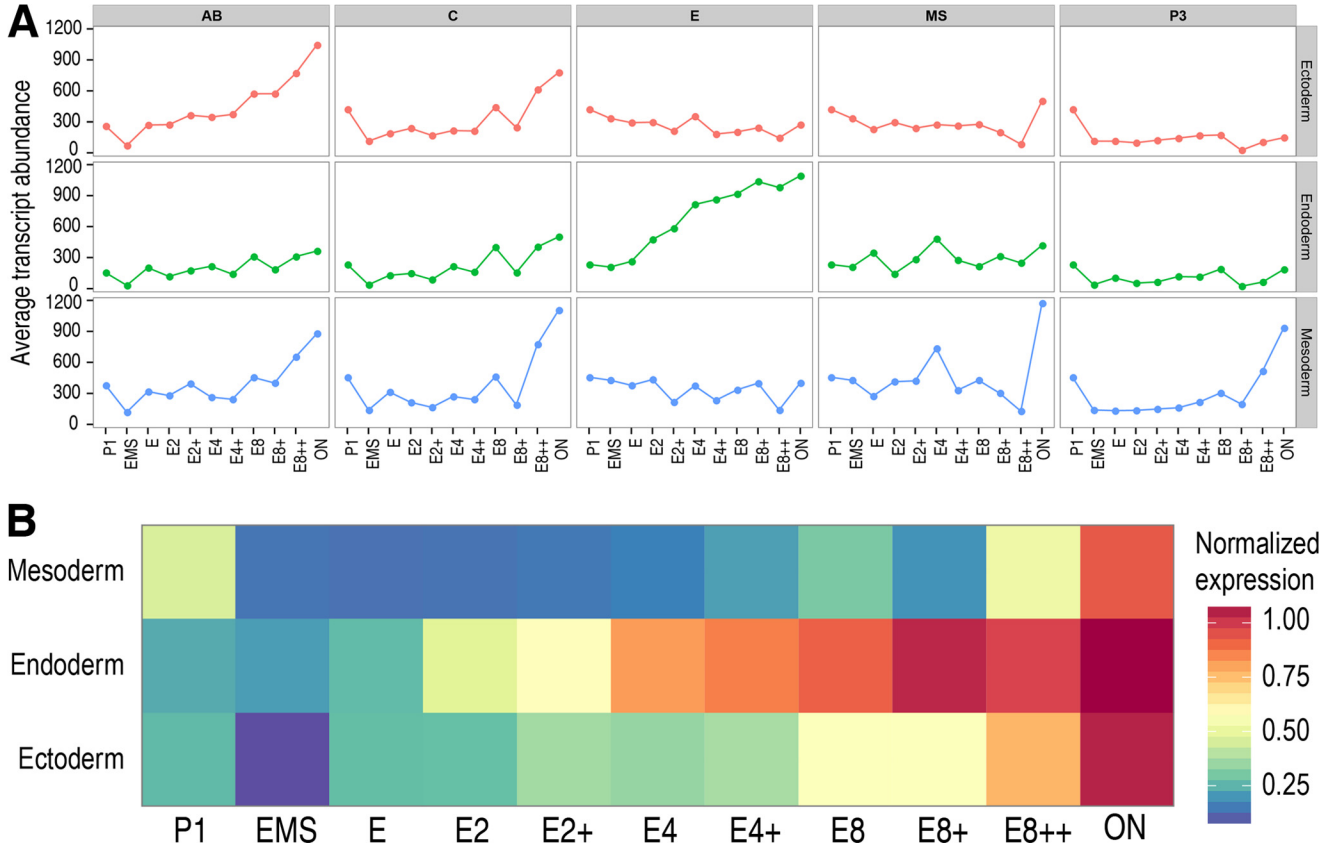

FIGURE 4. **Robust onset of gene expression is earlier in E-derived endoderm lineage than in other germ layers derived from AB, MS, C, and P3 lineages.** *A,* expression dynamics of germ layer-specific genes in progeny derived from various blastomeres. Transcript abundance (rpkm on *vertical axis*) is plotted against development time (*horizontal axis*) aligned with E, P1, and EMS. P1, EMS, E, E2, E4, and E8 denote their birth times; *E2+* denotes time when MSa and MSp complete division; *E4+* denotes 60 min after birth of E4 cell; *E8+* and *E8++* denote 90 and 180 min after birth of E8 cells. *ON*, overnight after E8. *B,* heat map showing germ layer-specific expression dynamics. Normalized transcripts for mesoderm, endoderm, and ectoderm are derived from P3, E, and AB, respectively.

also in AB8 cells in *C. elegans* (32). This raises the possibility that *wee-1.1* may provide some leverage for control of the E2-specific cell cycle, for example by E-specific fate specifiers, but itself may not specifically regulate E2 cell cycle length. Notably, except for *wee-1.1*, a significant reduction in the E2 cell cycle length was not observed in the genetic hypomorphic or conditional allele of the remaining tested genes whose perturbation gave rise to a shortened E2 cell cycle length by RNAi (supplemental Table S2). This is likely due to an incomplete depletion of their gene product in genetic allele compared with RNAi. Taken together, the results indicate distinct control over cell cycle length between E2 and other cells during *C. elegans* embryogenesis.

Endoderm Demonstrates an Earlier Activation of Robust Transcription than Other Germ Layers That Coincide with Elongation of E2 Cell Cycle Length—Given a differential requirement of gene transcription for division timing between endoderm and other germ layers, we hypothesized that an elongated E2 cell cycle could be due to an earlier onset of zygotic transcription in endoderm than in other germ layers. To test the hypothesis, we mined the previous lineage-specific RNA-seq data over nematode embryogenesis (23). As expected, the expression data demonstrated an earlier onset of zygotic transcription in E-derived endoderm than in the other two germ layers, *i.e.* MS-derived mesoderm and AB-derived ectoderm. To align the expression onset relative to E2 division timing, we plotted the average expression level for the genes that were shown to be germ layer-specific based on previous tissue-specific profiling data (33) over developmental time using divisions of E and its daughters as a reference whenever it is available (see "Materials and Methods") (Fig. 4). The data show a substantial increase of zygotic expression in E2 but not in E, suggesting a robust zygotic expression is not initiated in E until its division into E2. In contrast, zygotic expression in the other two germ layers does not reach a similar scale until E8 or E8++ stage for ectoderm and endoderm, respectively, suggesting a much later initiation of robust expression therein. It is worth noting that the magnitude of expression is much higher in E progeny than those in mesoderm and ectoderm, suggesting initiation of a strong and robust expression program is required for an extended E2 cell cycle in wild-type embryo (Fig. 4*B*), which is consistent with previous results (19, 34).

Regulation of E2 Cell Cycle Length Can Be Coupled with or Independent of Intestine Fate Differentiation—Intestine fate specification and E2 cell cycle extension occur simultaneously during *C. elegans* embryogenesis. This raises the question of whether the two developmental processes are genetically coupled. Study of E2 cycle length in the presence and absence of *wee-1.1* demonstrated that these events are at least partially separable from one another (30). This is based on the observation that a shortened E2 cell cycle length caused by a loss-of-function in *wee-1.1* is not accompanied by a loss of expression

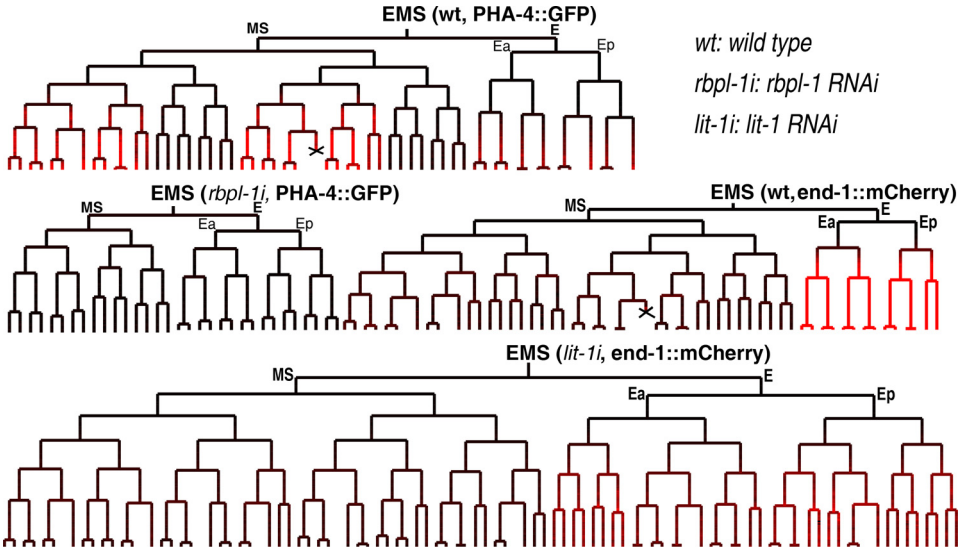

FIGURE 5. **Significant reduction in E2 cell cycle length can be coupled with or separated from cell fate specification.** *Top,* EMS lineage tree from a wild-type embryo with PHA-4 expression colored in *red*. *Middle left,* EMS lineage tree from an *rbpl*-1 RNAi embryo that shows a simultaneous reduction in E2 cell cycle length and loss of PHA-4 expression. *Middle right,* EMS lineage tree from a wild-type embryo with END-1 expression colored in *red*. *Bottom,* an EMS lineage tree from a *lit*-1 RNAi embryo, Note a transformation from E to MS-like fate, but the expression of *end-1* reporter is retained. Cell deaths are indicated with an "*X*".

of intestine markers. We previously showed that a gain-of-function in the cell cycle-promoting phosphatase, CDC-25.1, also produced a reduced E cell cycle length starting from E4 without changing the expression of the intestine marker (3), supporting a separate regulation between the E cell cycle and intestine fate specification.

However, as expected, knockdown of *rbpl-1* along with other components of general transcription machinery not only reversed the extended cell cycle length observed in E progeny in a wild-type embryo but also erased fate differentiation as judged by a loss of expression of the fate marker, PHA-4, in both MS and E lineage and early embryonic arrest (Fig. 5) as well as a decrease in lineage marker expression (supplemental Fig. S1), suggesting the regulation of E2 cell cycle length and intestine fate differentiation converges at gene transcription. In contrast, a loss-of-function in Wnt signaling pathway components, for example LIT-1 or MOM-2 (Table 1), resulted in a similar change in cell cycle length of E progeny as that for *rbpl-1* knockdown (Figs. 2*A* and 3*B*), but the intestine fate was properly differentiated based on the END-1 expression. The results indicate that the intestine fate differentiation could be either separated from or coupled with the regulation of E2 cell cycle length.

wee-1.1 May Function Upstream of General Transcription Machinery in Regulating E2 Cell Cycle Length—Given that both a loss-of-function in *wee-1.1* and inhibition of general transcription or its regulators could lead to a significant decrease in E2 cell cycle length, it would be essential to determine whether these genes function in the same or different pathways. To this end, we first quantified the E2 cell cycle length in the wild-type or *wee-1.1* loss-of-function background by automated lineage. We next measured the E2 cell cycle lengths by individually knocking down two components of general transcription machinery in the *wee-1.1* null background, including *rbpl-1* and D1081.8, which are predicted to be involved in mRNA poly(A) tailing and pre-RNA splicing, respectively (27). We found that the E2 cell cycle lengths were comparable upon knockdown of the two components regardless of the presence or absence of the WEE-1.1 (Fig. 6). However, in both cases the phenotypes of *wee-1.1* were masked by RNAi against either *rbpl-1* or D1081.8 suggesting that *wee-1.1* regulates the E2 cell cycle length upstream of RBPL-1 and D1081.8. CBP-1 is a homolog of the mammalian transcriptional cofactors CBP and p300, which have been shown to possess histone acetyltransferase activity. Knockdown of *cbp-1* resulted in a reduction in E2 cell cycle length parallel to the depletion of many components involved in general transcription (Table 1). However, the E2 cell cycle length change caused by CBP-1 depletion was partially rescued by a loss-of-function in *wee-1.1* (Fig. 6), suggesting that *cbp-1* regulates E2 cell cycle length upstream of *wee-1.1* or the two function in redundant pathways in regulating E2 cell cycle length.

Defective E2 Cell Cycle Length Is Commonly Associated with Cell Migration Defects and a Gastrulation Failure—A genetic screen for temperature-sensitive mutants with reversal of gonad handedness identified a gene, *gad-1*, with its name derived from the gastrulation defective mutation, which resulted in a failure of gastrulation (15). Perturbation of GAD-1 also led to precocious division of E2, suggesting a link between E2 division timing and gastrulation. To evaluate whether the defects in E2 cell cycle length picked up in our screening impair cell migration, we plotted the division angles of Ea and Ep for both wild-type and mutant embryos. Specifically, we first normalized the size and shape for all embryos (see under "Materials and Methods"). We then projected the division angles of all wild types and a subset of mutant embryos in a single three-dimensional space. We observed that for 46 out of the 76 genes with a significant decrease in E2 cell cycle length upon perturbation ($p < 0.05$), both Ea and Ep division angles were significantly deviated from the predominantly left-right (LR) axis as observed in 91 wild-type embryos (Fig. 7, *A* and *B*). Similarly, we

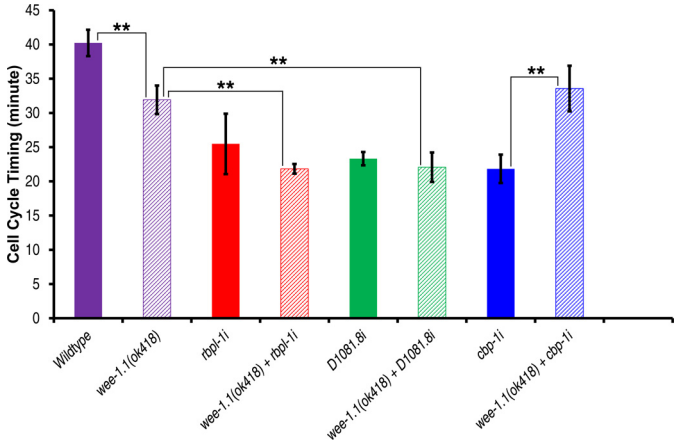

FIGURE 6. **Genetic interaction between *wee-1.1* and three genes whose perturbation leads to a significant reduction in E2 cell cycle length.** E2 cell cycle length is shown on *y* axis in minutes; genotypes are shown on *x* axis with "RNAi" abbreviated as "*i*". *wee-1.1* (−/−) contains allele *ok418*. A significant change ($p < 0.01$) is indicated by *two asterisks*.

plotted Ea and Ep cell positions in a single three-dimensional space and observed a significant deviation of the positions in mutant embryos from wild-type for 56 out of the 76 genes (Fig. 7, *C* and *D*). Notably, all of the embryos showing abnormal division angles are a subset of those with defective positions (Fig. 7*E*). The positional defects are also manifested as a displacement of Ea and Ep from its starting and ending time point (supplemental Fig. S2). As expected, a significant reduction in E2 cell cycle length is commonly associated with a failure in gastrulation (supplemental Fig. S3 and Movie S1 and S2), suggesting precise division timing is essential for proper E2 migration.

Discussion

How cell division pace is coordinated among one another during the proliferative stage of metazoan embryogenesis is a fundamental question in metazoan developmental biology. However, a molecular understanding of genetic control over embryonic cell division timing has only begun to emerge. Cell division during early embryogenesis has been thought to be mainly under maternal control. Consistent with this, a *C. elegans* embryo is able to achieve embryonic division up to 87 cells with few effects on asynchrony in the presence of the RNA polymerase II inhibitor, α-amanitin (12). However, inhibition of RNA polymerase II activities with its antisense RNA blocks the onset of *C. elegans* gastrulation and leads to a precocious division of E2 cells (13), suggesting a role of zygotic transcription in controlling division timing of embryonic cells. In agreement with this, activation of zygotic transcription is associated with a loss of cell cycle synchrony at the MBT stage of *Xenopus* embryogenesis (35). Unlike embryogenesis of *Xenopus laevis*, *Danio rerio*, and *Drosophila melanogaster*, where the initial rounds of cell division are synchronous and bulk activation of zygotic transcription only occurs after cell division begins to slow (11), *C. elegans* embryogenesis demonstrates abundant asynchronies between cells giving rise to the same or distinct cell type(s) from the very first cell division (2). A candidate approach identified ATL-1 and CHK-1, the *C. elegans* homologs of ATR (ATM and Rad3-related Protein) and Chk1 checkpoint kinases, respectively, which contribute to the observed asynchrony (36). We have recently performed a targeted reverse genetic screen with a focus on genetic control over asymmetry between sibling cells, and we demonstrated that a similar genetic architecture is in use for both division asynchrony and fate asymmetry during the proliferative stage of *C. elegans* embryogenesis (10). However, the asynchronies are not only found between sibling cells but are also observed for specific lineage or tissue. How asynchrony forms in a tissue- or lineage-specific way remains largely unknown.

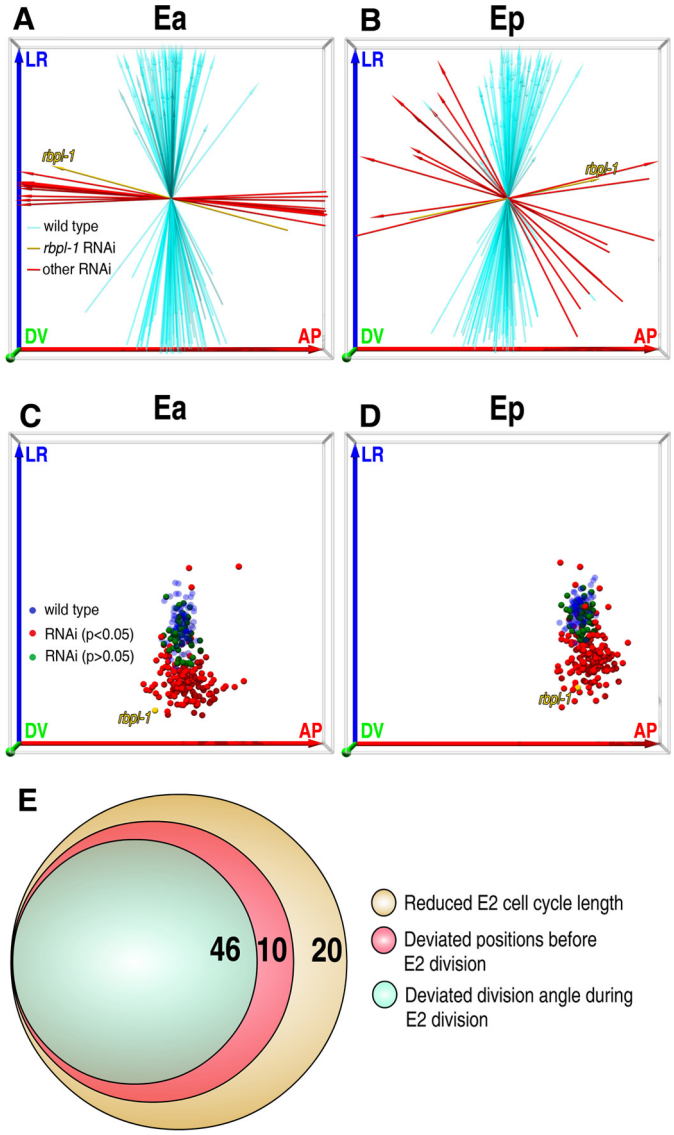

FIGURE 7. **Cell migrations associated with significantly faster E2 division ($p < 0.01$).** *A* and *B*, comparison of division angles of Ea and Ep, respectively, between the average of 91 wild-type embryos (*cyan*) and RNAi embryos perturbed with 11 genes (colored in *red* except for *rbpl-1* in *yellow*). The 11 genes are prioritized with the smallest *p* values of deviation from LR axis. *AP*, anterior-posterior; *LR*, left-right; *DV*, dorsal-ventral. All lines are normalized to unit vectors, to emphasize the angles. *C* and *D*, cell positions from wild-type and perturbed embryos. Genes with a significant ($p < 0.05$) or insignificant ($p > 0.05$) deviation of cell position from wild-type average (*blue*) are colored in *red* and *green*, respectively. The positions of *rbpl-1*(RNAi) embryos are shown in *yellow*. *E*, Venn diagram showing the number of genes that have a significant reduction in E2 cell cycle length (*yellow*), deviations in cell position (*red*), and division angle (*cyan*).

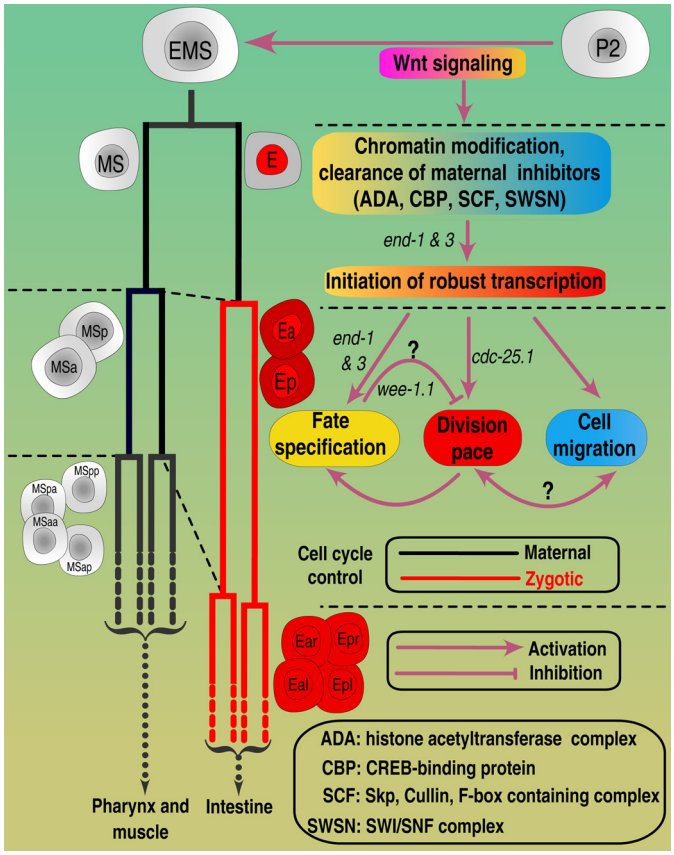

FIGURE 8. **Model of genetic control on E2 cell cycle length.** Wnt signaling along with maternal factors (not shown) triggers zygotic initiation of gene transcription in E through chromatin remodeling and histone modification as well as clearance of maternal inhibitors of transcription, which makes E transcriptionally ready and produces a few E fate specifiers, including END-1 and END-3. Robust gene transcription is up and running starting at E2, which is essential not only for intestine fate specification but also for an extension of E2 cell cycle length probably by introduction of G_2 gap stage, although control of cell cycle length in other cells is mainly under maternal control at the same stage. The controlled cell division timing is presumably important for proper cell migration, but the exact relationship between the two remains to be determined. Known cell cycle regulators involved in the E2 cell cycle control are shown.

Here, we provide evidence that tissue/lineage-specific regulation of cell cycle length requires a differential onset of gene transcription, which is supported by lineage-specific RNA-seq analysis (23). Identification of numerous components of the general transcription pathway or its regulators such as those involved in chromatin modification suggests that an earlier onset of transcription in E is triggered by the Wnt signaling pathway, which is likely to be followed by a combination of chromatin modification and clearance of maternal factors that inhibit transcriptional activation (Fig. 8). The requirement of activation of zygotic transcription for a delayed cell cycle is surprising because a general assumption is that active transcription is necessary for cell cycle progression. For example, division of the germ line precursor, P4, is substantially delayed compared with its cousins (2), because it remains transcriptionally quiescent until its division into Z2 and Z3 (37, 38), suggesting a robust transcription is necessary for driving cell cycle progression.

A prevailing model on cell cycle control during embryogenesis is the volume ratio between nucleus and cytoplasm termed as the N/C ratio (39). Under this model, a decreasing N/C ratio is responsible for the slowing cell cycle during a later stage of embryogenesis (35, 40). This is based on the observation that a decreased N/C ratio is accompanied by a titration of maternal factors that may inhibit the zygotic activation of transcription. Apparently, the model cannot account for the E2-specific cell cycle delay in *C. elegans* because the cell cycle length and cell volume follow a power law relationship in the AB, MS, C, and P lineages but not in E whose daughters exhibit an abrupt deviation from the common law obeyed by the remaining cells (41). One possible explanation is that delay is evolved to facilitate gastrulation. First, gastrulation occurs during the E2 stage, and E2 cells divide right after completion of ingression (Fig. 1, *B* and *C*). Second, a substantial decrease in E2 cell cycle length in a perturbed embryo is commonly associated with gastrulation delay or failure. Third, mis-regulated E2 cell cycle length is also associated with abnormal E2 division angles (Fig. 7). A previous study on DNA replication and gene transcription demonstrated that the G2 gap stage was introduced during the E2 lifetime (42). We speculate that the specific activation of zygotic expression in E2 cells is probably used for introducing the gap stage, although this seems not the case in zebrafish (43). Consistent with this, many of our perturbed embryos demonstrated an E2 cell cycle length of around 20 min (Table 1), which is roughly the time used for DNA synthesis (42). Future work should investigate the exact relationship between the initiation of zygotic transcription and gap/checkpoint introduction. It is also interesting to study how regulatory pathways, such as Wnt signaling, interface with cell cycle regulation. For example, does the signaling pathway regulate E2 cell cycle length by controlling the cell cycle checkpoint or by regulating the frequency of DNA replication firing through chromatin remodeling or histone modification?

In contrast, evidence shows that cell cycle length also plays a role in zygotic gene activation. For example, chemical inhibition of either DNA replication or the cell cycle progression results in precocious expression of zygotic transcripts in *Xenopus* (44). Similarly, interphase arrest induces premature transcription at cell cycle 10 in *D. melanogaster* (45). Transcription and cell proliferation remain synchronized during *C. elegans* embryogenesis when the overall developmental rate is changed by a temperature shift or a *clk-1* (*qm30*) background. However, expression of fate markers, including a gut marker ELT-2 and a muscle marker UNC-120 or HLH-1, is independent of cell cycle progression in the presence of *emb-29* (*g52*) or *div-1* (*or148*), respectively (20). Whether an increased E2 cell cycle length contributes to the activation of zygotic transcription in *C. elegans* remains to be determined. Given our criteria in prioritizing genes for perturbation, the genes that are involved in specific control of E2 cell cycle length but produce an otherwise normal embryo upon perturbation could be missed in our screening.

Study of genetic interaction between a component of the general transcription pathway, D1081.8, which is predicted to encode an RNA splicing factor, and a G_2/M checkpoint component, *wee-1.1* suggests that the latter regulates cell cycle by controlling gene transcription. However, the ability of a loss-of-function allele in *wee-1.1* in rescuing E2 cell cycle defect pro-

duced by CBP-1 depletion indicates that CBP-1 regulates E2 cell cycle by controlling *wee-1.1* activities. Given that the CBP-1 homolog in *Drosophila* was shown to respond to Wnt signaling for turning on gene expression (46), it is possible that the Wnt signaling pathway regulates the E2 cell cycle through CBP-1, which further controls *wee-1.1* activities. In agreement with this, although *wee-1.1* is expressed not only in daughters of E but also in daughters of AB (30, 32), only E2 cells receive the signal. Taken together, we propose a model for E2-specific cell cycle control (Fig. 8), in which Wnt signaling activates E2-specific gene expression by changing chromatin modification, probably through ADA-2, CBP-1, and SWSN-1, which in turn initiates the expression of intestine-specific factors, such as END-1 and END-3 in E. Previous study also revealed a requirement of chromatin regulators for cell cycle progression (9). Expression of the cell cycle negative regulator *wee-1.1* may function in synergy with degradation of the cell cycle-promoting phosphatase CDC-25.1 by the SCF (Skr-Cullin-F box) complex in elongating the E2 cell cycle length. Thus, the controlled E2 cell division timing may facilitate its migration in the context of a developing embryo. Although differential expression of F-box that is responsible for CDC-25.2 degradation appears to contribute to its intestine-specific degradation (47), how *wee-1.1* plays an E-specific role in regulating cell cycle length remains unclear. It would be intriguing to investigate whether *wee-1.1* is a direct target of *end-1* and *end-3*. The exact relationship between E2 division pace and cell migration remains to be determined.

Author Contributions—Z. Z. conceived and coordinated the study and wrote the paper. M. K. W., V. W. S. Z., X. A., and X. R. performed the experiments. M. K. W. contributed to manuscript writing. D. G., R. L., and K. H. C. N. performed data analysis. All authors reviewed the results and approved the final version of the manuscript.

Acknowledgments—We thank Chung Wai Shing for logistic support and the members of the Zhao lab for helpful discussion and comments, in particular Khandker Khaldun Islam for critical reading of the manuscript. Some strains were provided by the CGC, which is funded by National Institutes of Health, Office of Research Infrastructure Programs, Grant P40 OD010440.

References

1. Dong, P., Maddali, M. V., Srimani, J. K., Thélot, F., Nevins, J. R., Mathey-Prevot, B., and You, L. (2014) Division of labour between myc and G1 cyclins in cell cycle commitment and pace control. *Nat. Commun.* **5,** 4750
2. Sulston, J. E., Schierenberg, E., White, J. G., and Thomson, J. N. (1983) The embryonic cell lineage of the nematode *Caenorhabditis elegans*. *Dev. Biol.* **100,** 64–119
3. Bao, Z., Zhao, Z., Boyle, T. J., Murray, J. I., and Waterston, R. H. (2008) Control of cell cycle timing during *Caenorhabditis elegans* embryogenesis. *Dev. Biol.* **318,** 65–72
4. Tavernier, N., Labbé, J. C., and Pintard, L. (2015) Cell cycle timing regulation during asynchronous divisions of the early *Caenorhabditis elegans* embryo. *Exp. Cell Res.* **337,** 243–248
5. Gonczy, P, and Rose, L. S. (2005) Asymmetric cell division and axis formation in the embryo. *WormBook 2005*, 1–20
6. Rose, L., and Gonczy, P. (2014) Polarity establishment, asymmetric division and segregation of fate determinants in early *Caenorhabditis elegans* embryos. *WormBook 2014*, 1–43
7. Bao, Z., Murray, J. I., Boyle, T., Ooi, S. L., Sandel, M. J., and Waterston, R. H. (2006) Automated cell lineage tracing in *Caenorhabditis elegans*. *Proc. Natl. Acad. Sci. U.S.A.* **103,** 2707–2712
8. Murray, J. I., Bao, Z., Boyle, T. J., Boeck, M. E., Mericle, B. L., Nicholas, T. J., Zhao, Z., Sandel, M. J., and Waterston, R. H. (2008) Automated analysis of embryonic gene expression with cellular resolution in *Caenorhabditis elegans*. *Nat. Methods* **5,** 703–709
9. Krüger, A. V., Jelier, R., Dzyubachyk, O., Zimmerman, T., Meijering, E., and Lehner, B. (2015) Comprehensive single cell-resolution analysis of the role of chromatin regulators in early *Caenorhabditis elegans* embryogenesis. *Dev. Biol.* **398,** 153–162
10. Ho, V. W., Wong, M. K., An, X., Guan, D., Shao, J., Ng, H. C., Ren, X., He, K., Liao, J., Ang, Y., Chen, L., Huang, X., Yan, B., Xia, Y., Chan, L. L., *et al.* (2015) Systems-level quantification of division timing reveals a common genetic architecture controlling asynchrony and fate asymmetry. *Mol. Syst. Biol.* **11,** 814
11. Lee, M. T., Bonneau, A. R., and Giraldez, A. J. (2014) Zygotic genome activation during the maternal-to-zygotic transition. *Annu. Rev. Cell Dev. Biol.* **30,** 581–613
12. Edgar, L. G., Wolf, N., and Wood, W. B. (1994) Early transcription in *Caenorhabditis elegans* embryos. *Development* **120,** 443–451
13. Powell-Coffman, J. A., Knight, J., and Wood, W. B. (1996) Onset of *Caenorhabditis elegans* gastrulation is blocked by inhibition of embryonic transcription with an RNA polymerase antisense RNA. *Dev. Biol.* **178,** 472–483
14. Maduro, M. F., Broitman-Maduro, G., Mengarelli, I., and Rothman, J. H. (2007) Maternal deployment of the embryonic SKN-1→MED-1,2 cell specification pathway in *Caenorhabditis elegans*. *Dev. Biol.* **301,** 590–601
15. Knight, J. K., and Wood, W. B. (1998) Gastrulation initiation in *Caenorhabditis elegans* requires the function of gad-1, which encodes a protein with WD repeats. *Dev. Biol.* **198,** 253–265
16. Bowerman, B., Eaton, B. A., and Priess, J. R. (1992) Skn-1, a maternally expressed gene required to specify the fate of ventral blastomeres in the early *Caenorhabditis elegans* embryo. *Cell* **68,** 1061–1075
17. Zhu, J., Hill, R. J., Heid, P. J., Fukuyama, M., Sugimoto, A., Priess, J. R., and Rothman, J. H. (1997) End-1 encodes an apparent GATA factor that specifies the endoderm precursor in *Caenorhabditis elegans* embryos. *Genes Dev.* **11,** 2883–2896
18. Maduro, M. F., Meneghini, M. D., Bowerman, B., Broitman-Maduro, G., and Rothman, J. H. (2001) Restriction of mesendoderm to a single blastomere by the combined action of SKN-1 and a GSK-3β homolog is mediated by MED-1 and -2 in *Caenorhabditis elegans*. *Mol. Cell* **7,** 475–485
19. Boeck, M. E., Boyle, T., Bao, Z., Murray, J., Mericle, B., and Waterston, R. (2011) Specific roles for the GATA transcription factors end-1 and end-3 during *Caenorhabditis elegans* E-lineage development. *Dev. Biol.* **358,** 345–355
20. Nair, G., Walton, T., Murray, J. I., and Raj, A. (2013) Gene transcription is coordinated with, but not dependent on, cell divisions during *Caenorhabditis elegans* embryonic fate specification. *Development* **140,** 3385–3394
21. Shao, J., He, K., Wang, H., Ho, W. S., Ren, X., An, X., Wong, M. K., Yan, B., Xie, D., Stamatoyannopoulos, J., and Zhao, Z. (2013) Collaborative regulation of development but independent control of metabolism by two epidermis-specific transcription actors in *Caenorhabditis elegans*. *J. Biol. Chem.* **288,** 33411–33426
22. Zhao, Z., Flibotte, S., Murray, J. I., Blick, D., Boyle, T. J., Gupta, B., Moerman, D. G., and Waterston, R. H. (2010) New tools for investigating the comparative biology of *Caenorhabditis briggsae* and *Caenorhabditis elegans*. *Genetics* **184,** 853–863
23. Hashimshony, T., Feder, M., Levin, M., Hall, B. K., and Yanai, I. (2015) Spatiotemporal transcriptomics reveals the evolutionary history of the endoderm germ layer. *Nature* **519,** 219–222
24. McGhee, J. D., Sleumer, M. C., Bilenky, M., Wong, K., McKay, S. J., Goszczynski, B., Tian, H., Krich, N. D., Khattra, J., Holt, R. A., Baillie, D. L., Kohara, Y., Marra, M. A., Jones, S. J., Moerman, D. G., *et al.* (2007) The ELT-2 GATA-factor and the global regulation of transcription in the *Caenorhabditis elegans* intestine. *Dev. Biol.* **302,** 627–645
25. Zhao, Z., Boyle, T. J., Liu, Z., Murray, J. I., Wood, W. B., and Waterston,

R. H. (2010) A negative regulatory loop between microRNA and hox gene controls posterior identities in *Caenorhabditis elegans*. *PLoS Genet.* **6,** e1001089
26. Lin, R., Thompson, S., and Priess, J. R. (1995) Pop-1 encodes an HMG box protein required for the specification of a mesoderm precursor in early *Caenorhabditis elegans* embryos. *Cell* **83,** 599–609
27. Yook, K., Harris, T. W., Bieri, T., Cabunoc, A., Chan, J., Chen, W. J., Davis, P., de la Cruz, N., Duong, A., Fang, R., Ganesan, U., Grove, C., Howe, K., Kadam, S., Kishore, R., *et al.* (2012) WormBase 2012: More genomes, more data, new website. *Nucleic Acids Res.* **40,** D735–D741
28. Bowerman, B., Ingram, M. K., and Hunter, C. P. (1997) The maternal par genes and the segregation of cell fate specification activities in early *Caenorhabditis elegans* embryos. *Development* **124,** 3815–3826
29. Yang, Q., and Ferrell, J. E., Jr. (2013) The Cdk1-APC/C cell cycle oscillator circuit functions as a time-delayed, ultrasensitive switch. *Nat. Cell Biol.* **15,** 519–525
30. Robertson, S. M., Medina, J., and Lin, R. (2014) Uncoupling different characteristics of the *Caenorhabditis elegans* E lineage from differentiation of intestinal markers. *PLoS ONE* **9,** e106309
31. Broitman-Maduro, G., Maduro, M. F., and Rothman, J. H. (2005) The noncanonical binding site of the MED-1 GATA factor defines differentially regulated target genes in the *Caenorhabditis elegans* mesoderm. *Dev. Cell* **8,** 427–433
32. Wilson, M. A., Hoch, R. V., Ashcroft, N. R., Kosinski, M. E, and Golden, A. (1999) A *Caenorhabditis elegans* wee1 homolog is expressed in a temporally and spatially restricted pattern during embryonic development. *Biochim. Biophys. Acta* **1445,** 99–109
33. McGhee, J. D., Fukushige, T., Krause, M. W., Minnema, S. E., Goszczynski, B., Gaudet, J., Kohara, Y., Bossinger, O., Zhao, Y., Khattra, J., Hirst, M., Jones, S. J., Marra, M. A., Ruzanov, P., Warner, A., *et al.* (2009) ELT-2 is the predominant transcription factor controlling differentiation and function of the *Caenorhabditis elegans* intestine, from embryo to adult. *Dev. Biol.* **327,** 551–565
34. Maduro, M. F., Broitman-Maduro, G., Choi, H., Carranza, F., Wu, A. C., and Rifkin, S. A. (2015) MED GATA factors promote robust development of the *Caenorhabditis elegans* endoderm. *Dev. Biol.* **404,** 66–79
35. Newport, J., and Kirschner, M. (1982) A major developmental transition in early *Xenopus* embryos: II. control of the onset of transcription. *Cell* **30,** 687–696
36. Brauchle, M., Baumer, K., and Gönczy, P. (2003) Differential activation of the DNA replication checkpoint contributes to asynchrony of cell division in *Caenorhabditis elegans* embryos. *Curr. Biol.* **13,** 819–827
37. Seydoux, G., and Strome, S. (1999) Launching the germline in *Caenorhabditis elegans*: Regulation of gene expression in early germ cells. *Development* **126,** 3275–3283
38. Seydoux, G., and Dunn, M. A. (1997) Transcriptionally repressed germ cells lack a subpopulation of phosphorylated RNA polymerase II in early embryos of *Caenorhabditis elegans* and *Drosophila melanogaster*. *Development* **124,** 2191–2201
39. Edgar, B. A., Kiehle, C. P., and Schubiger, G. (1986) Cell cycle control by the nucleo-cytoplasmic ratio in early *Drosophila* development. *Cell* **44,** 365–372
40. Newport, J., and Kirschner, M. (1982) A major developmental transition in early *Xenopus* embryos: I. characterization and timing of cellular changes at the midblastula stage. *Cell* **30,** 675–686
41. Arata, Y., Takagi, H., Sako, Y., and Sawa, H. (2014) Power law relationship between cell cycle duration and cell volume in the early embryonic development of *Caenorhabditis elegans*. *Front. Physiol.* **5,** 529
42. Edgar, L. G., and McGhee, J. D. (1988) DNA synthesis and the control of embryonic gene expression in *Caenorhabditis elegans*. *Cell* **53,** 589–599
43. Dalle Nogare, D. E., Pauerstein, P. T., and Lane, M. E. (2009) G_2 acquisition by transcription-independent mechanism at the zebrafish midblastula transition. *Dev. Biol.* **326,** 131–142
44. Kimelman, D., Kirschner, M., and Scherson, T. (1987) The events of the midblastula transition in *Xenopus* are regulated by changes in the cell cycle. *Cell* **48,** 399–407
45. Edgar, B. A., and Schubiger, G. (1986) Parameters controlling transcriptional activation during early *Drosophila* development. *Cell* **44,** 871–877
46. Li, J., Sutter, C., Parker, D. S., Blauwkamp, T., Fang, M., and Cadigan, K. M. (2007) CBP/p300 are bimodal regulators of Wnt signaling. *EMBO J.* **26,** 2284–2294
47. Hebeisen, M., and Roy, R. (2008) CDC-25.1 stability is regulated by distinct domains to restrict cell division during embryogenesis in *Caenorhabditis elegans*. *Development* **135,** 1259–1269